PHYSICAL REVIEW B VOLUME 23, NUMBER 12 15 JUNE 1981

Calculation of the formation entropy and diffusivity constants for the vacancy in Mg

A. M. Monti and E. J. Savino
Departamento Materiales, Comisión Nacional de Energía Atómica, Buenos Aires, Argentina
(Received 8 December 1980)

By assuming a pair interatomic potential which reproduces some Mg properties, we calculate the formation entropy for a vacancy in an hcp lattice. A value of that entropy between 1.5 and $2k$ is obtained at variance with previous experimental findings which favor a very small value. By a quasistatic computer-simulation approach the migration energies for the vacancy on different lattice directions are also calculated; two different potentials are used for this calculation. Subsequently migration entropies and diffusivities are evaluated. A good agreement with reported experimental values is obtained. Diffusion in hcp structures is space anisotropic, and the relative influence on this anisotropy of the migration energy with respect to the entropy is discussed.

I. INTRODUCTION

The study of the micro- and macroscopic behavior of hcp metals is always involved, due to the intrinsic crystal anisotropy. This anisotropy is generally enhanced as the lattice-parameter ratio c/a separates from the rigid-sphere packing value $[c/a = (8/3)^{1/2}]$. However, even for Mg, with a c/a ratio of 1.6237, very near the ideal one, the value of most physical quantities depends on the crystal orientation. For example, Janot *et al.*[1] tried to obtain the vacancy-formation energy and entropy by measuring the macroscopic and lattice thermal dilation of Mg single crystals. These authors found not only a strong anisotropy in those dilations but they inferred a formation-energy value for the vacancy of 0.58 eV which differs strongly from those deduced previously by resistivity measurements[2] and diffusivity.[3] These latter values are larger, in the range of 0.78–0.93 eV. Also Janot *et al.* report a very small vacancy-formation entropy $(0 \pm 0.3k)$. This value is, however, very difficult to determine experimentally even for the comparatively isotropic cubic metals where the formation energy for the vacancy is relatively well known. In Mg, single-crystal diffusivity measurements are reported by Shewmon[3] and Combronde and Brebec.[4] These authors found that tracer diffusion in a direction perpendicular to the crystal c axis was faster than in the parallel direction. Shewmon attributed the difference to the entropy contribution in the vacancy migration. By contrast, Combronde *et al.*, basing their considerations on a simple model, ascribed it to a difference in migration energies. This anisotropic behavior of the self-diffusion coefficient is larger for other hcp metals with a different c/a ratio (see Adda and Philibert[5] for a review).

A deeper theoretical understanding of the statics and dynamics of the relevant lattice defects therefore seems necessary in order to clarify the above experimental findings. This involves the development of detailed atomic models which, although more or less empirical, retain enough information about some lattice properties and above all about the proper lattice symmetry. As we have argued in a previous paper[6] the similarity between lattice defects in fcc and hcp metals may cause one to overlook some relevant differences. On the other hand, as discussed by Hatcher *et al.*,[7] the theoretical predictions of the vacancy-formation entropy, even in a well studied metal such as Cu, give widely diverging results and, as pointed out by Lidiard,[8] the calculation of migration entropies has been relatively neglected in the literature. Hatcher *et al.*[7] recently performed a self-consistent pair-potential calculation of the vacancy and divacancy formation energies and entropies together with the self-diffusion constants for cubic Cu and α-Fe. A similar study is reported here for the vacancy and its migration in the hcp Mg.

The distortion around the vacancy in the static Mg lattice has already been calculated by several authors.[6,9-11] In the paper of Tomé *et al.*[6] two different pair interatomic potentials were discussed. Both have a relatively short range; one, called EP hereafter (for "empirical potential"), is a cubic spline chosen to give a vacancy-formation energy of 0.8 eV and to reproduce approximately the Mg elastic constants, while the other, SP (for "pseudopotential"), is based on the ion interaction part of the optimized pseudopotential deduced by Appapillai and Heine.[12] However, the vacancy-formation energy calculated through this potential is 0.24 eV,[6] the rest in principle being contributed by the electron-gas volume-dependent term. For the EP the rigid-sphere packing c/a ratio is adopted while for the SP $c/a = 1.6237$. In most of the calculations reported below the EP is used because of its shorter range that allows for quicker convergency and its appropriate adjustment to the vacancy-formation energy. The SP is only used

for making comparisons at constant volume.

The plan of the present paper is as follows. In Sec. II we calculate the vacancy-formation entropy. Then in Sec. III the vacancy diffusivity in the hexagonal-close-packed structure is discussed and the migration energies and entropies as well as the isotope factors are calculated for Mg. Finally the diffusivity is calculated and in Sec. IV the theoretical findings are compared with the experimental ones.

II. VACANCY-FORMATION ENTROPY

A. Theory

Here we follow the work of Hatcher *et al.*[7] The entropy S is there divided into a vibrational part S^v and an electronic contribution S^e. They found the electronic contribution to be negligible except for materials with a large density of states at the Fermi energy. We concentrate then in the vibrational contribution. The formation entropy for the defect is

$$S_1 \simeq S_1^v = \frac{k}{2} \ln\left(\prod_{\alpha=1}^{3N} (\omega_\alpha^0)^2 \Big/ \prod_{\alpha=1}^{3N} (\omega_\alpha)^2 \right), \tag{1}$$

in the classical limit of high temperatures, where ω_α refers to the α eigenfrequency of the defect lattice and ω_α^0 to that of the perfect lattice. As, by forming the vacancy, the atom at the now vacant site is transferred to the surface, both lattices contain the same number N of atoms and therefore $3N$ eigenfrequencies. Some authors have calculated (1) for the vacancy in Cu within an Einstein approximation,[13,14] where each atom is allowed to vibrate in the potential well created by the equilibrium configuration of neighboring atoms. However, coupling terms may make a large contribution to the entropy.[15] Also the appropriate lattice relaxation and boundary corrections may be relevant. Hatcher *et al.*[7] favor a determinant method, which includes coupling terms and lattice relaxation and in which

$$S_1^v = \frac{k}{2} \ln(\det\phi^0 / \det\phi), \tag{2}$$

ϕ being the $3N \times 3N$ force-constant matrix of the perfect (ϕ^0) and defect (ϕ) lattice. The influence of elastic and surface correction is also discussed in Ref. 7 and it will be considered by us below (Sec. IIC).

We shall next, in Sec. IIB, deduce an explicit expression for the vacancy-formation entropy in an unrelaxed hcp structure within a first-neighbor Einstein approximation. Thereafter, the atomic coordinates, obtained by allowing numerical relaxation of a region with approximately 2000 atoms held together by the EP and bounded by a perfect hcp lattice,[6] are used for the entropy calculations. Within that region, N atoms around the vacant site are allowed to vibrate while the remaining atoms are held fixed at their relaxed sites. Both the Einstein approximation, Sec. IIB, and the determinant method, Eq. (2), Sec. IIC, are used in order to calculate the entropy. A comparison of the results obtained by either method allows us to assess the relative influence of the coupling components. The results are extrapolated to $N \to \infty$; therefore, within the validity of that extrapolation, long-range effects are explicitly included in the calculation.

B. Einstein approximation

If only a first-neighbor-range interaction is allowed in the unrelaxed lattice, then the equation for vacancy-formation entropy agrees with that deduced, under the same assumptions, by Hatcher *et al.*[7] for fcc lattices,

$$S_1^v = 6k \ln \frac{(4f_l + 8f_t)^3}{(3f_l + 8f_t)(4f_l + 7f_t)^2}. \tag{3}$$

Here f_l and f_t are, respectively, the longitudinal and transverse force constants. For the EP at the first neighbor $f_t/f_l = 9 \times 10^{-3}$. Under the assumption $f_t = 0$, Eq. (3) is potential independent and $S_1^v = 1.73k$.

If the defect-lattice configuration which results from computer simulation[6] is adopted, Eq. (1) can be calculated within the Einstein approximation by allowing for the vibration of N relaxed atoms, each one within the potential well created by all neighbors within the EP range. The calculated values depend on the number N of atoms. Some of these values are reported in Fig. 1 as a function of $1/N$. The entropy seems for large N to average a value of $S_1^v = 1.55k$ which is 10% smaller than the one obtained assuming first-neighbor interaction and no relaxation.

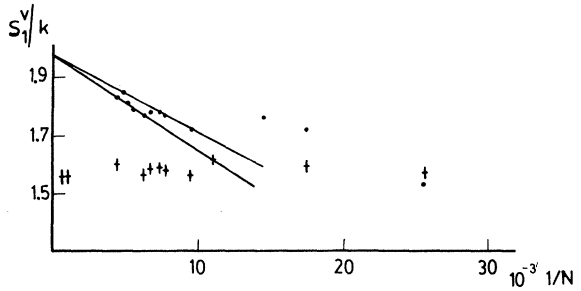

FIG. 1. Formation entropy of the vacancy as a function of $1/N$, where N is the number of atoms allowed to vibrate. •: Determinant approximation, Eq. (2). +: Einstein approximation.

C. Determinant method

By using Eq. (2), where the determinant of the force-constant matrix for N atoms within the relaxed lattice region must be calculated, the collective vibration modes of those atoms are explicitly included in the calculation of the vacancy-formation entropy. The main difficulty with this method is computer storage and time. For example, our present computer facility does not allow us to handle more than approximately 250 atoms. Even then, the calculation for that number of atoms requires the evaluation of the determinant of a 750×750 matrix.

Perfect and defect lattice differ in (i) the vacant site at the origin of the last one, plus (ii) an extra atom at the surface and (iii) the displacement of all remaining atoms for minimizing the energy. Although both lattices show equal numbers of vibration modes, equal-*size* finite regions which include the origin lack three vibration modes in the defect lattice with respect to the perfect one. As $(\det\phi)$ depends on the size and shape of the region, equivalent regions for either lattice have to be used for calculating S_1 and the difference in the number of normal modes has to be either weighted or the lacking modes properly included. However, the influence of three modes is smeared out for large N and the error introduced for any approximation adopted for those modes should be small. Hatcher *et al.*[7] propose to evaluate the determinant for the available atoms within a region and then to multiply the perfect-lattice $\ln(\det\phi^0)$ value by $(N-1)/N$. The same approach is adopted by us in what follows. Also, the above-mentioned authors show that the calculated formation entropy for N atoms $S_1^v(N)$ converges to the one $S_1^v(\infty)$ for an infinite number of atom as

$$S_1^v(N) = S_1^v(\infty) + \text{const}/N . \tag{4}$$

In Fig. 1 we plot the values of Eq. (2) with the above-mentioned correction against $1/N$, the inverse of the number of atoms included in the calculation of $\det\phi$. Although there is some influence of the region shape for different values of N, it can be seen that $S_1^v(N)$ approximately converges to a value $S_1^v(\infty) \simeq 1.97k$.

The vacancy-formation entropy calculated above should be accurate for a crystal of approximately 5 000 atoms (these included in the relaxed and unrelaxed regions for the computer simulation), hold together by the EP with a *displacement-free* surface. Real crystals are generally larger and bounded by a *force-free* surface. Eshelby, as referred to in Ref. 13, suggests the thermodynamic relation

$$S_1|_P = S_1|_V + K\alpha\Delta V , \tag{5}$$

to correct the above-calculated constant-volume entropy (more accurately the *constant-lattice-parameter* entropy) with respect to the "true," constant-pressure, formation entropy. (This relation was pointed out to us by Lidiard, and it is also reviewed by Flynn.[16]) In (5) K stands for the experimental bulk modulus and α for thermal expansion while ΔV should be the calculated relaxation volume. We have found that, even for the vacancy case, there is always some error in determining that volume.[17] However, for the EP calculations by using the method proposed by Schober and Ingle,[18] a value of $\Delta V/\Omega \simeq -0.1$ is obtained; therefore we calculate for $(S_1|_P - S_1|_V) \simeq -0.16k$.

III. VACANCY DIFFUSION IN AN hcp CRYSTAL

A. Diffusivity in hcp lattices

The diffusivity in an hcp lattice is anisotropic. If diffusion takes place by a vacancy mechanism the tracer can either jump to a vacant site located in the same basal plane, with a rate ω_{B_0}, or to one located outside that plane, with a rate ω_{A_0}. In Fig.

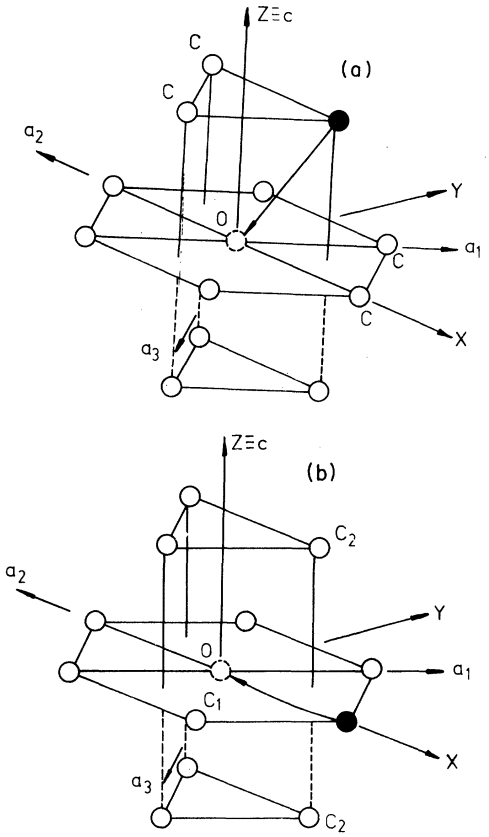

FIG. 2. Scheme of the two possible tracer-vacancy jumps in an hcp structure. Dotted sphere: vacant site. Shaded sphere: tracer (a) A_0 jump; (b) B_0 jump.

2 the two jumps are schematically shown. The tracer diffusion has one component parallel to the c axis,

$$D_{\parallel} = \tfrac{3}{4} c^2 f_{Az_0} \omega_{A_0}, \tag{6a}$$

and a different one perpendicular to it,

$$D_{\perp} = \tfrac{3}{2} a^2 f_{Bx_0} \omega_{B_0} + \tfrac{1}{2} a^2 f_{Ax_0} \omega_{A_0}, \tag{6b}$$

where f are the correlation factors. For self-diffusion these factors have been deduced by Combronde and Brebec,[4] based on the work of Ghate,[19] and they depend on the ratio $r = \omega_{B_0}/\omega_{A_0}$, which is itself temperature dependent. The jump rates are

$$\omega_{A_0, B_0} = \left(\frac{\omega^*_{A_0, B_0}}{2\pi}\right) \exp\left(\frac{S_1}{k}\right) \exp\left(-\frac{E_0 + H_{A_0, B_0}}{kT}\right), \tag{7}$$

where E_0 is the vacancy-formation energy, H_{A_0, B_0} the migration energy for the A_0 or B_0 jump and, from Vineyard's theory,[20] the frequency ω^* is

$$\omega^* = \frac{\prod_{\alpha=1}^{3N} \omega^e_\alpha}{\prod_{\alpha=1}^{3N-1} \omega^s_\alpha}, \tag{8}$$

where ω^e_α are the eigenfrequencies for the defect lattice with an equilibrium vacant site, while ω^s_α are those for the saddle-point configuration; in the product at the bottom of (8) the eigenfrequency for the unstable mode $[(\omega^s_{un})^2 < 0]$ is excluded. Evidently two different saddle points have to be considered for the A_0 and B_0 jumps. The frequency ω^* may be written as[16]

$$\omega^* = \omega_0 \exp(\Delta S_m / k), \tag{9}$$

where ω_0 is arbitrary. This is often taken as the Einstein eigenfrequency of an atom first neighbor to the vacancy and vibrating towards it. It is assumed to account for the number of attempts made by the atom per unit time for crossing the potential barrier to the vacancy. ΔS_m defined by (8) and (9) is the motion entropy.

B. Vacancy migration energy

The defect migration barrier can be computer simulated within a quasistatic approximation. This amounts to assuming that the defect migration is composed of successive $3N$-dimension configurations in the space of atomic displacements, such that, for each of those configurations, $3N$ relaxed force-constant eigenvalues with their corresponding eigenvectors can be found where only one is unstable while the perpendicular $(3N-1)$ hyperplane is in equilibrium. A similar procedure is adopted by Johnson,[21] Ingle and Crocker,[22] and Sinclair and Fletcher.[23] The latter have adapted the conjugate-gradient method for saddle-point localization. Within the quasistatic approximation we shall calculate the barrier for the vacancy migration by creating a nearest-neighbor divacancy conveniently oriented. Thereafter an extra lattice atom is located as an interstitial between the two vacant sites but not allowing its displacement towards the nearest vacancy in order to prevent recombination. The $(3N-1)$ coordinates that remain free (i.e., those which do not include the projection of the interstitial coordinates on the direction of the vacancy) are allowed to relax in order to minimize the energy under either the EP or the SP interaction. "Trial and error" is employed in order to find the minimum-energy path, i.e., the minimum-energy sequence of $(3N-1)$-dimension hyperplanes above defined where the migration path is determined by the perpendicular $3N$-dimension-displacements eigenvector, corresponding to a negative eigenvalue of the relaxed force-constant matrix. That displacement sequence allows the interstitial to move from one vacant site to the other. Approximately 2000 atoms are allowed to relax and both the EP and the SP are used for the simulation.

Even for a rigid-sphere-packing c/a ratio, where the jump distance is the same for the A_0 or the B_0 jump, their saddle-point configuration is quite different.[3,4] For A_0, the jumping atom when located midway between the two vacant sites has four first neighbors, marked as C in Fig. 2, while for the B_0 jump the three atoms, named C_1 and C_2 in Fig. 2, constitute the main barrier for the migration. As a consequence of the lattice symmetry, the saddle-point location of the jumping atom in the A_0 jump is at the center of the rectangle determined by the C atoms, which should relax keeping that center invariant. In contrast, for the B_0 jump, the only lattice symmetry that has to be kept by the jumping atom is to remain within the same basal plane. There remains at least one degree of freedom for the saddle-point configuration which is not determined by the lattice symmetry and which is therefore potential dependent. For the sake of giving some description of the saddle-point configurations we report in Table I the calculated displacement of the above-mentioned C, C_1, and C_2 atoms together with the location of the tracer atom at the saddle point. For the calculation of the B_0 jump which uses the EP, the saddle point is found not to be for the jumping atom at an equidistant location between the two vacant sites; actually, as discussed below, when it is there, local equilibrium is created. In Table I some atom locations for that equilibrium configuration are also reported.

The energy barrier for migration is calculated in the quasistatic approximation mentioned above.

TABLE I. Saddle-point configuration for the vacancy migration.

Jump	Jumping atom	Atom named in Fig. 2	Neighbor atoms: Perfect lattice location (a)	Neighbor atoms: Displacement (a)	Potential used for the calculation
A_0 $\left(\frac{a}{2},\frac{a}{2\sqrt{3}},\frac{c}{2}\right)\rightarrow(0,0,0)$	$\left(\frac{a}{4},\frac{a}{4\sqrt{3}},\frac{c}{4}\right)$	C	$(1,0,0)$	$(0.043,-0.003,-0.013)$	EP
				$(0.055,-0.003,-0.033)$	SP
B_0 $(a,0,0)\rightarrow(0,0,0)$	$\left(\frac{a}{2},-0.17a,0\right)$[a]	C_1	$(1/2,-\sqrt{3}/2,0)$	$(0.0,-0.114,0)$[a]	EP
		C_2	$(1/2,1/2\sqrt{3},c/2a)$	$(0.0,0.002,0.011)$[a]	
	$\left(\frac{a}{2},-0.09a,0\right)$	C_1	$(1/2,-\sqrt{3}/2,0)$	$(0,-0.112,0)$	SP
		C_2	$(1/2,1/2\sqrt{3},c/2a)$	$(0.0,0.023,0.030)$	
	$(0.56a,-0.15a,0)$	C_1	$(1/2,-\sqrt{3}/2,0)$	$(-0.016,-0.102,0)$	EP
		C_2	$(1/2,1/2\sqrt{3},c/2a)$	$(-0.005,-0.001,0.014)$	

[a] Local equilibrium configuration for the EP calculation (see text).

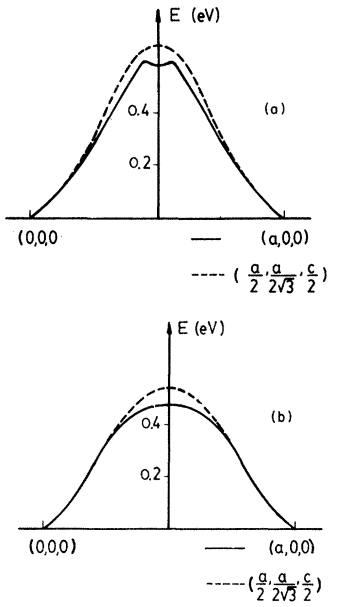

FIG. 3. Migration energy for the vacancy. (a) EP; (b) SP.

The energy values are plotted in Fig. 3 against the distance from the jumping-atom relaxed location to its original site, now vacant (or, more accurately, against the projection of that distance into the straight line joining the jumping-atom site before the jump with its site after the jump). It can be seen that for the B_0 jump calculation with the EP, the above-mentioned local equilibrium configuration appears for the jumping atom located midway between those locations. Its existence is further confirmed by calculating the eigenfrequencies of this configuration which are all real. The calculated maxima in the energy barrier for the A_0 and B_0 jumps are reported in Table II together with the values deduced in Ref. 4 from the experimental data. It can be seen that, although the calculations with the two different potentials predict different absolute values for the energy-barrier-maximum H (as expected due to the above-mentioned difference in their predictions of vacancy-formation energy), both sets predict H_{A_0} to be larger than H_{B_0} and the same difference (δH) between values. This result seems to show an influence of the lattice symmetry on the migration energy which is independent of the potential used for the calculation.

TABLE II. Energy barrier for vacancy migration.

H_{A_0} (eV)	H_{B_0} (eV)	δH (eV)	Reference
0.66	0.59	0.07	EP
0.54	0.47	0.07	SP
0.59	0.57	0.02	Experimental, Ref. 4

C. Vacancy migration entropy

The migration frequency defined by Eq. (8) must now be calculated. For the calculation procedure we find it useful to rewrite (8) as

$$\omega^* = \mathrm{Im}\left(\omega^s_{\mathrm{un}} \exp \frac{\delta S_m - S_1^v}{k}\right), \tag{10}$$

where δS_m is defined as a parameter to be calculated as

$$\delta S_m = \frac{k}{2} \ln \left(- \frac{\prod_{\alpha=1}^{3N} (\omega^0_\alpha)^2}{\prod_{\alpha=1}^{3N} (\omega^s_\alpha)^2} \right), \tag{11}$$

and S_1^v was defined in (1). For the calculation of δS_m the $3N$ eigenfrequencies of both the perfect lattice (ω^0_α) and the saddle-point configuration (ω^s_α) are used, the unstable one—$(\omega^s_{\mathrm{un}})^2 < 0$—being included. The minus sign within the ln function in Eq. (11) compensates for this negative value. Both the unstable frequency ω^s_{un} and the eigenfrequencies necessary for obtaining the parameter δS_m can be calculated within either the Einstein or the determinant approximations as discussed for the vacancy-formation entropy. Some eigenfrequencies ω^s_{un} calculated by using the EP are reported in Table III. To evaluate the unstable eigenfrequency within the determinant approximation involves finding the eigenvalues of relatively large matrices. Computer time did not allow us to go into the eigenvalue calculation beyond the

TABLE III. Unstable eigenfrequencies and ΔK factors for vacancy migration.

N	$-i\omega^s_{\mathrm{un}A_0}$ (10^{13} sec^{-1})	ΔK_{A_0}	$-i\omega^s_{\mathrm{un}B_0}$ (10^{13} sec^{-1})	Δ_{B_0}	Method
1	1.62	1	1.59	1	Einstein
12	1.97	0.92	1.86	0.87	Determinant
38	2.12	0.86	2.28	0.80	
68	2.27	0.82	2.30	0.80	
86	2.27	0.82	2.30	0.80	

number of atoms reported in that table. However, convergence seems to have been obtained. By using the EP interaction we have calculated δS_m, Eq. (11), within the Einstein approximation for a varying number of atoms and extrapolated the values $\delta S_{mA_0} = 3.5k$ and $\delta S_{mB_0} = 3.0k$. From these values together with $S_1 = 1.55k$, there results: $\omega^*_{A_0} = 1.1 \times 10^{14}$ sec^{-1} and $\omega^*_{B_0} = 6.8 \times 10^{13}$ sec^{-1} Within the determinant approximation

$$\delta S_m = \frac{k}{2}\left(\frac{N-1}{N}\ln(\det\phi^0) - \ln(-\det\phi^s)\right). \tag{12}$$

This quantity is plotted as a function of $1/N$ and extrapolated to $1/N \to 0$ in Fig. 4 ($\delta S_{mA_0} = 7.3k$, $\delta S_{mB_0} = 4.5k$). From those extrapolated values and the unstable eigenfrequencies of Table III one obtains $\omega^*_{A_0} \simeq 5.3 \times 10^{15}$ sec^{-1} and $\omega^*_{B_0} \simeq 3.2 \times 10^{14}$ sec^{-1}. If the attempt jump frequency, ω_0 in Eq. (9), for a near-neighbor atom to a vacancy is calculated within the Einstein approximation there results $\omega_{0A_0} \simeq \omega_{0B_0} \simeq \omega_0 = 2.9 \times 10^{13}$ sec^{-1}. Then, the migration entropies are calculated as $\Delta S_{mA_0} = 1.33k$, $\Delta S_{mB_0} = 0.85k$, for δS_m obtained within the Einstein approximation, and $\Delta S_{mA_0} = 5.21k$, $\Delta S_{mB_0} = 2.40k$ if Eq. (12) is used for δS_m. The entropy ratio is then about 2 while the energy ratio is $H_{A_0}/H_{B_0} = 1.1$.

Both the frequencies ω^* and the entropies ΔS_m have been obtained at constant lattice-parameter-boundary condition. For referring those values to constant pressure, "true"-crystal variables, a correction equivalent to the one in Eq. (5), must be included. This correction is proportional to the difference between the saddle-point and the equilibrium-vacancy relaxation volumes and it has also been discussed by Flynn.[16] Our calculation of the saddle-point relaxation volume is, however, affected by a relatively large numerical error,[17] and an approximate correction of $-0.5k$ results for the migration entropy in either jump. This value is perhaps too large and, surprisingly, it is negative, but one must not forget that the

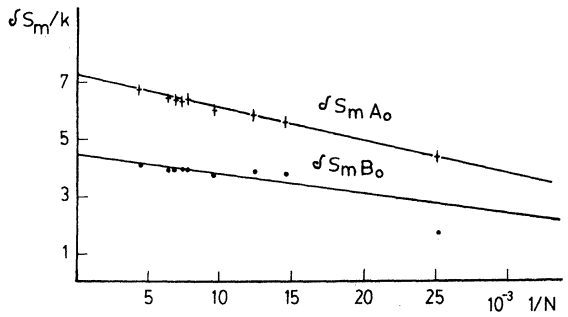

FIG. 4. Equation (12) is plotted for the A_0 and B_0 jumps as a function of $1/N$, where N is the number of atoms used for the calculation.

volume-relaxation value, on which it depends, has been found[6] to be strongly potential dependent. The above-mentioned volume-relaxation correction is used for calculating within the determinant approximation the ω^* values needed in Sec. III E for diffusivity calculations.

D. Isotope factor

The isotope factor ΔK is generally defined by the change of ω^*:

$$\frac{\delta\omega^*}{\omega^*} = -\frac{1}{2}\frac{\delta M}{M}\Delta K, \tag{13}$$

when a tracer isotope with mass $M + \delta M$ is used for diffusion with respect to its values for one of mass M. ΔK can be calculated within our model as[7]

$$\Delta K = (U^T_{3N})^2, \tag{14}$$

where U^T_{3N} is the normalized eigenvector of the ϕ^s matrix corresponding to the unstable frequency ω^s_{un}. Those factors calculated by using the EP are reported in Table III together with their corresponding ω^s_{un}. It can be seen that they seem to converge to a value of approximately 0.8 even for relatively few atoms and ΔK_{A_0} seems to be slightly larger than ΔK_{B_0}.

E. Diffusivity calculation

Throughout this section and the preceding section we have calculated all the parameters necessary for evaluating expressions (5) and (6). Two self-consistent approximations have been applied for all the calculations that involve atomic vibration modes: the Einstein and the determinant one. Equations (5) and (6) can then be calculated within either approximation. We do so in the range 500–640°C, which is that used experimentally, and compare in Fig. 5 the theoretical predictions with the experimental values obtained by Combronde and Brebec[4] by measuring the residual activity. It can be seen that the diffusivities obtained within either approximation show the correct activation energy. Also those obtained within the Einstein approximation show the correct ratio $D_\perp/D_\parallel$, though their separate values are one order of magnitude smaller than the experimental. On the other hand, the diffusivities obtained within the determinant approximation appear to have the correct order of magnitude but the incorrect ratio $D_\perp/D_\parallel$, $D_\parallel$ being almost twice $D_\perp$. If the calculated diffusivities are represented by a straight line, values of activation energies Q and D_0 [$D_0 = D(1/T)$, $1/T \to 0$] are obtained. Those are reported in Table IV.

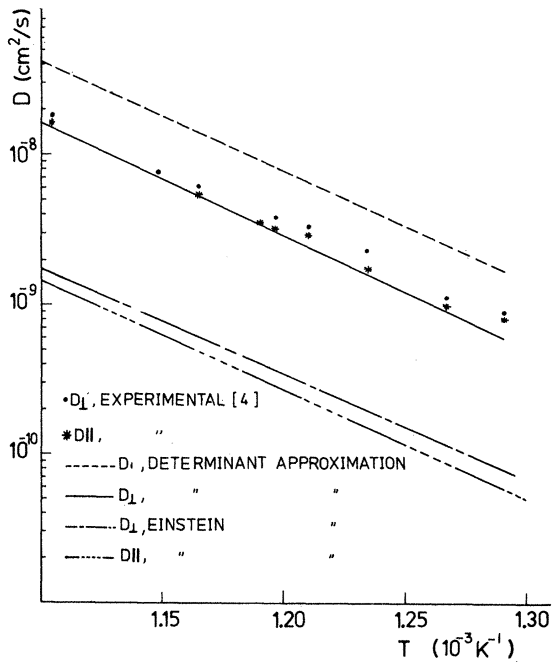

FIG. 5. Experimental and calculated diffusivities as a function of $1/T$.

IV. SUMMARY AND CONCLUSIONS

In this paper we have used a pair-interaction-potential model to calculate the following properties of vacancies in Mg:

(i) The vacancy-formation entropy, where the vibrational contribution was considered and surface and boundary corrections included through thermodynamic relations.

(ii) The migration energy of the vacancy within and outside the basal plane; H_{B_0}, H_{A_0}.

(iii) The unstable vibration eigenfrequencies at the saddle-point configurations and the related ΔK factors.

(iv) The migration frequencies ω^*, Eq. (8), which are related to the migration entropy ΔS_m by Eq. (9).

(v) Finally, the diffusivity constants due to vacancy migration in an hcp single crystal $D_\perp$ and $D_\parallel$ were calculated in the same temperature range as the experimental measurements reported in the literature.

(vi) From those diffusivity values the activation energies for diffusion $Q_\perp$ and $Q_\parallel$ and the $D_{0\perp}$ and $D_{0\parallel}$ factors are deduced.

We want now to comment on the above-mentioned results. Our calculation predicts a vacancy-formation entropy for Mg of approximately $1.8k$. This differs from the only value we have found in the literature,[1] where a very small value for this entropy was obtained. It is hard for us to understand how this entropy can be close to zero if, as previously discussed, its main contribution is due to lattice vibrations. We have seen that the vacancy first neighbors alone contribute $\simeq 1.7k$ to the entropy without allowing for their relaxation, assuming $f_t = 0$. A great deal of cancellation must take place to compensate for that value. In our model, relaxation plus the inclusion of cooperative modes increase this value while the boundary condition of constant pressure reduces it. Also it can be pointed out that by comparing the formation entropy calculated within the Einstein approximation even for a relative large number of atoms, with the one resulting from the more accurate determinant method, the coupling among vibration modes gives a contribution of over 15% of the total. In the case of the migration entropy (Sec. III C) the differences between the results of the two approximations show that neglecting coupling terms in the Einstein approximation substantially underestimates the entropy values.

The migration energies calculated by using the EP agree fairly well with those reported in the literature. The resulting activation energy H_{A_0} of the nonbasal vacancy jump A_0 is found to be larger than that of the basal jump H_{B_0}. Their difference seems to be more sensitive to the different saddle-point configurations than to the potential assumed for the atomic interaction. It is also interesting that the calculated migration entropy is larger for the nonbasal than for the basal jump, independent of the approximation (Einstein or determinant) used for the calculation. This result agrees with Zener's early prediction[24]

TABLE IV. Activation energy for diffusion and D_0 values.

$D_{0\parallel}$ (cm²/sec)	$D_{0\perp}$ (cm²/sec)	$Q_\parallel$ (eV)	$Q_\perp$ (eV)	Method	Reference
1.0	1.5	1.40	1.41	Experimental	3
1.78	1.75	1.44	1.43	Experimental	4
0.18	0.11	1.46	1.41	Theory, Einstein	this work
4.69	1.38	1.46	1.45	Theory, determinant	this work

that larger migration energy implies also larger migration entropy. The calculated constant-volume migration-entropy values are relatively large, and this finding contradicts Flynn's assumption[16] that the motion entropy must originate principally in the volume dependence of the phonon frequencies.

Concerning the calculated diffusivity values we can say that in view of the large number of approximations used for the calculation it is quite encouraging to find sensible values for that parameter. On the other hand, as stated above we found anisotropic values both in the migration energy and entropy for the vacancy jump. The first one favors a vacancy jump perpendicular to the c axis while the second favors the opposite one. The measured anisotropy must be a consequence of the relative values of those parameters. Therefore, for the calculation which uses the Einstein approximation for entropy calculations, a ratio $D_\perp/D_\parallel$ which agrees with the experimental findings is obtained while for the determinant method, which should be more accurate, an incorrect ratio is obtained. However the calculated diffusivity is closer to the experimental values if this last method is used.

ACKNOWLEDGMENTS

We want to thank P. H. Dederichs for suggesting some of the calculations and for very interesting discussions, A. B. Lidiard for carefully reading the manuscript and for his clarifying comments and the IAEA for supporting Dederichs's visit to our group. Finally, one of us (E.J.S.) wants to thank Professor A. Salam, the IAEA and UNESCO for hospitality at the International Center for Theoretical Physics, Trieste, while writing the manuscript. This work was partly supported by a grant from Comisión de Investigaciones Cientificas de la Provincia de Buenos Aires (CIC).

[1]C. Janot, D. Malléjac, and B. George; Phys. Rev. B 2, 3088 (1970).
[2]C. Mairy, J. Hillairet, and D. Schumacher, Acta Metall. 15, 1258 (1967).
[3]P. G. Shewmon, Trans. Metall. Soc. AIME 206, 918 (1956).
[4]J. Combronde and G. Brebec, Acta Metall. 19, 1393 (1971).
[5]Y. Adda and J. Philibert, *La Diffusion dans les Solides* (Universite de France Press, 1966).
[6]C. N. Tomé, A. M. Monti, and E. J. Savino, Phys. Status Solidi B 92, 323 (1979).
[7]R. D. Hatcher, R. Zeller, and P. H. Dederichs, Phys. Rev. B 19, 5083 (1979).
[8]A. B. Lidiard, in *Theory of Imperfect Crystalline Solids-Trieste Lectures, 1970* (I. A. E. A., Vienna, 1971), p. 339.
[9]Z. D. Popovic and J. P. Carbotte, J. Phys. F 4, 1599 (1974).
[10]M. Doneghan and P. T. Heald, Phys. Status Solidi B 30, 403 (1975).
[11]D. Sahoo and H. K. Sahu, Phys. Rev. B 18, 6738 (1978).
[12]M. Appapillai and V. Heine, Tech. Report No. 5 SST/7/1972 Cambridge University, 1972 (unpublished).
[13]H. B. Huntington, G. A. Shirn, and E. S. Wajda, Phys. Rev. 99, 1085 (1955).
[14]P. Wynblatt, J. Phys. Chem. Solids 30, 2395 (1969).
[15]G. F. Nardelli and N. Tettamanzi, Phys. Rev. 126, 1283 (1962).
[16]C. P. Flynn, *Point Defects and Diffusion* (Clarendon, Oxford, 1972).
[17]A. M. Monti and E. J. Savino, in *Fifth Interamerican Conference on Materials Technology*, edited by Departmento de Publicações do Instituto de Pesquisas Tecnológicas do Estado de Saõ Paulo-IPT (Gráfica Editora, Hamburg Ltda; 1978), p. 13.
[18]H. R. Schober and K. W. Ingle, J. Phys. F 10, 575 (1980).
[19]P. B. Ghate, Phys. Rev. 133, A 1167 (1964).
[20]G. H. Vineyard, J. Phys. Chem. Solids 3, 121 (1957).
[21]R. A. Johnson, Phys. Rev. 134, 1329 (1964).
[22]K. W. Ingle and A. G. Crocker, Philos. Mag. A 37, 297 (1978).
[23]J. E. Sinclair and R. Fletcher, J. Phys. C 7, 864 (1974).
[24]C. Zener, in *Imperfections in Nearly Perfect Crystals*, edited by W. Shockley *et al.* (Wiley, New York, 1952), p. 295.